A small-molecule antagonist of CXCR4 inhibits intracranial growth of primary brain tumors

Joshua B. Rubin*†‡§, Andrew L. Kung*‡¶, Robyn S. Klein‖**, Jennifer A. Chan*†,††, YanPing Sun‡‡, Karl Schmidt‡‡, Mark W. Kieran*, Andrew D. Luster‖, and Rosalind A. Segal*†§§

Departments of *Pediatric Oncology and ¶Cancer Biology, Dana–Farber Cancer Institute, Boston, MA 02115; ‖Center for Immunology and Inflammatory Diseases, Massachusetts General Hospital, Charlestown, MA 02129; ††Department of Pathology, Children's Hospital, Boston, MA 02115; ‡‡Department of Radiology, Brigham and Women's Hospital, Boston, MA 02115; and †Department of Neurobiology, Harvard Medical School, Boston, MA 02115

Communicated by Bruce M. Spiegelman, Harvard Medical School, Boston, MA, September 11, 2003 (received for review July 21, 2003)

The vast majority of brain tumors in adults exhibit glial characteristics. Brain tumors in children are diverse: Many have neuronal characteristics, whereas others have glial features. Here we show that activation of the G_i protein-coupled receptor CXCR4 is critical for the growth of both malignant neuronal and glial tumors. Systemic administration of CXCR4 antagonist AMD 3100 inhibits growth of intracranial glioblastoma and medulloblastoma xenografts by increasing apoptosis and decreasing the proliferation of tumor cells. This reflects the ability of AMD 3100 to reduce the activation of extracellular signal-regulated kinases 1 and 2 and Akt, all of which are pathways downstream of CXCR4 that promote survival, proliferation, and migration. These studies (*i*) demonstrate that CXCR4 is critical to the progression of diverse brain malignances and (*ii*) provide a scientific rationale for clinical evaluation of AMD 3100 in treating both adults and children with malignant brain tumors.

Malignant brain tumors are a major cause of cancer-related morbidity and mortality in both adults and children. Each year ≈15,000 patients die despite the best available multimodal therapy (1). The genetics of common adult and pediatric CNS malignancies, such as glioblastoma multiforme (GBM) and medulloblastoma, suggest that enhanced proliferation, increased resistance to apoptosis, and increased cell migration are all involved in the progression and maintenance of a cancerous state (2, 3). Thus, specific biological agents that simultaneously target all these processes may provide therapeutic alternatives to conventional cytotoxic therapies.

Chemokines, secreted factors initially described as regulators of leukocyte trafficking (4), are now known to have far-reaching influence in the development and functioning of many tissues. A critical role in the developing brain for the chemokine stromal cell-derived factor 1α (CXCL12) and its receptor, CXCR4, became evident when targeted gene deletion of either resulted in significant abnormalities in cerebellar development (5, 6). Cardinal features of the mutant animals were the mislocalization and failed proliferation of cerebellar granule precursor cells (GPCs). These phenotypic changes in GPCs reflect two effects of CXCL12, a chemotactic effect (7–9) and the ability of CXCL12 to synergize with Sonic hedgehog (Shh) in the promotion of GPC proliferation (7). The capacity of CXCL12 and CXCR4 to regulate proliferation and migration of neural precursor cells raises the possibility that these molecules might be therapeutic targets in malignancies arising from CNS progenitors.

CXCR4 expression in the brain is not limited to GPCs. Additional neuronal populations (10), astrocytes (11–13), and adult GBM all express CXCR4 (14–16). Here we report that CXCR4 mRNA and protein are expressed at high levels in brain tumors of both neuronal and astrocytic lineage. The ligand CXCL12 is expressed in tumor-associated blood vessels and/or tumor cells, suggesting a paracrine relationship for CXCR4 activation *in vivo*. *In vitro*, CXCL12 exerts proliferative, antiapoptotic, and chemotactic effects on both GBM and medulloblastoma cell lines. *In vivo*, systemic administration of AMD 3100, a small-molecule inhibitor of CXCR4 (17), decreased growth of GBM and medulloblastoma xenografts. Direct antitumor effects of AMD 3100 were evident in reduced activation of extracellular signal-regulated kinases 1 and 2 (Erk 1/2) and Akt and increased rates of apoptosis in both tumor types. Together these studies identify CXCR4 signaling as a critical component of brain tumor biology and demonstrate that small-molecule inhibition of CXCR4 has significant antineoplastic activity. AMD 3100 is well tolerated in human studies (18); thus, these findings could rapidly lead to clinical trials for malignant brain tumors.

Materials and Methods

Immunostaining. Cultured cells were fixed in 4% paraformaldehyde. Formalin-fixed paraffin-embedded human tumor sections were heated in 10 mM citrate, pH 6.0, for 30 min at 99°C before staining. Those specimens stained for platelet endothelial cell adhesion molecules (PECAM) were digested with 10 μg/ml trypsin (Sigma) for 3 min at room temperature. Antibodies used were as follows: anti-CXCL12, 400 ng/ml on fixed cells or 10 ng/ml for human specimens (PeproTech, Rocky Hill, NJ); anti-CXCR4, 2 μg/ml (R & D Systems) on fixed cells or 50 ng/ml for human specimens; anti-PECAM, 5 μg/ml (Pharmingen); anti-BrdUrd, 1 μg/ml (Roche Molecular Biochemicals); anti-pErk1/2, 1:100 (Cell Signaling Technology, Beverly, MA); anti-pAkt (Ser 473), 1:100 (Cell Signaling Technology); followed by secondary antibodies conjugated to horseradish peroxidase, FITC, or Cy3.

Cell Culture. U87 and Daoy cells (American Type Culture Collection) were cultured in DMEM with 10% FCS (GIBCO/BRL). Cells were treated with CXCL12 (PeproTech), platelet-derived growth factor (R & D Systems), Shh (Curis, Cambridge, MA), or AMD 3100 (AnorMED, Langley, BC, Canada) as indicated. To assess proliferation, cultured cells were pulsed for 4 h with 10 μM BrdUrd and analyzed by colorimetric BrdUrd ELISA (Roche Molecular Biochemicals). Apoptosis was assessed by terminal deoxynucleotidyltransferase-mediated dUTP nick end labeling (TUNEL) assay (Roche Molecular Biochemicals). Chemotaxis was evaluated with a 4-h Boyden microchemotaxis assay as described (7) by using polyvinylcarbonate-free

Abbreviations: GBM, glioblastoma multiforme; GPC, granule precursor cell; Shh, Sonic hedgehog; Erk 1/2, extracellular signal-regulated kinases 1 and 2; TUNEL, terminal deoxynucleotidyltransferase-mediated dUTP nick end labeling; PECAM, platelet endothelial cell adhesion molecules; SFM, serum-free media.

‡J.B.R. and A.L.K. contributed equally to this work.

§Present address: Department of Pediatrics, Washington University School of Medicine, St. Louis, MO 63110.

**Present address: Department of Internal Medicine, Washington University School of Medicine, St. Louis, MO 63110.

§§To whom correspondence should be addressed at: Dana–Farber Cancer Institute, 44 Binney Street, Boston, MA 02115. E-mail: rosalind_segal@dfci.harvard.edu.

membranes (Neuroprobe, Cabin John, MD) with 12-μm pore size and coated with 20 μg/ml laminin (Sigma). In some experiments, cells were pretreated with 200 ng/ml pertussis toxin (Sigma) for 1 h or preincubated with a CXCR4-blocking monoclonal antibody (Pharmingen) at 10 μg/ml.

Luciferase Expression. The coding sequences for luciferase and neomycin phosphotransferase were fused and introduced into a pMMP retrovirus (Richard Mulligan, Children's Hospital, Boston), generating pMMP-LucNeo. pMMP-LucNeo was packaged in 293T cells by cotransfection with plasmids encoding helper functions (from pMD murine leukemia virus) and vesicular stomatitis virus (VSV)-G envelope protein (pMD-G; Richard Mulligan). Pseudotyped VSV-G was applied to cells with 8 μg/ml polybrene (Sigma). LucNeo-expressing cells were selected with 1 mg/ml G418 (GIBCO/BRL).

Tumor Cell Line Xenografts. Tumor cell lines were harvested in midlogarithmic growth phase and resuspended in PBS. Homozygous NCR nude mice (Taconic Farms) were anesthetized with ketamine hydrochloride at 150 mg/kg and xylazine at 12 mg/kg (Phoenix Pharmaceuticals, St. Joseph, MO) i.p. before exposure of the cranium and removal of the periosteum with a size 34 inverted cone burr (Roboz, Gaithersburg, MD). Mice were fixed in a stereotactic frame (Stoelting), and 50,000 cells in 10 μl of PBS were injected through a 27-gauge needle over 2 min at 2 mm lateral and posterior to the bregma and 3 mm below the dura. The incision was closed with Vetbond (3M Co.).

***In Vivo* AMD 3100 Treatment.** Mice were imaged at least twice after implantation of cells to identify those in which tumor burden increased over time. Ten to 12 days after implantation of U87 cells and 4–6 weeks after implantation of Daoy cells, cohorts of 8–10 mice per experiment with approximately equivalent tumor bioluminescence were divided into equal control and treatment groups. Subcutaneous osmotic pumps (Alzet, Palo Alto, CA) loaded with 20–30 mg/ml AMD 3100 in sterile PBS or PBS alone were used according to the manufacturer's instructions. The infusion rate was 0.5 μl/h. Alternatively, animals were injected with 1.25 mg/kg AMD 3100 subcutaneously twice per day for the duration of treatment. Four hours before the mice were killed, BrdUrd at 400 mg/kg (Sigma) was injected i.p. Apoptosis in xenografts was measured by TUNEL assay (Roche Molecular Biochemicals). BrdUrd and TUNEL data are presented as percent positive nuclei (labeled tumor nuclei per total tumor nuclei $\times$ 100%).

***In Vivo* Imaging.** Mice were anesthetized, injected with D-luciferin at 50 mg/ml i.p. (Xenogen, Alameda, CA), and imaged with the IVIS Imaging System (Xenogen) for 10–120 s, bin size 2. To quantify bioluminescence, identical circular regions of interest were drawn to encircle the entire head of each animal, and the integrated flux of photons (photons per second) within each region of interest was determined by using the LIVING IMAGES software package (Xenogen). Data were normalized to bioluminescence at the initiation of treatment for each animal.

MRI Imaging. Mice were anesthetized with 1% isofluorane and received 0.8 ml/kg gadopentetate dimeglumine (Gd) i.p.; the mice were then imaged with an 8.5-T Biospec vertical bore system (Bruker, Billerica, MA). T_1-weighted, post-Gd images were obtained by using a repetition time of 1,000 ms, an echo time of 8.8 ms, a slice thickness of 0.75 mm, a matrix size of 128 $\times$ 128 cm, and a field of view of 2.56 $\times$ 2.56 cm^2. 3D-rendered, Gd-enhanced, T_1-weighted images were generated with in-house 3D software, and tumor volume was measured by using a thresholding method (19).

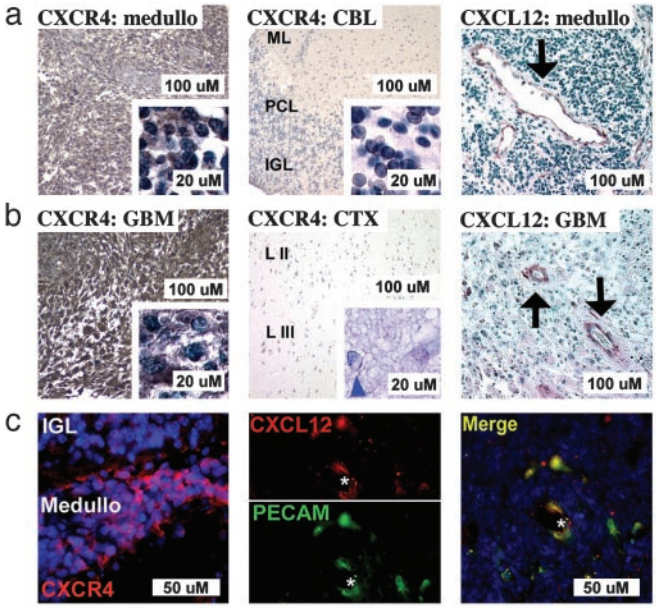

Fig. 1. CXCR4 and CXCL12 are expressed in human and mouse brain tumors. (*a*) CXCR4 immunoreactivity (brown) is in human medulloblastoma cells (*Left*) but not in cerebellar granule cells (*Center*). The low-magnification view (*Left*) shows a densely cellular tumor; the high-power view (*Inset*) shows that tumor cells are immunoreactive for CXCR4. The low-power view of the cerebellum (CBL) (*Center*) reveals a normal layered structure, internal granule cell layer (IGL), Purkinje cell layer (PCL), and molecular layer (ML); the high-power view (*Inset*) shows that granule cells of the IGL exhibit little to no CXCR4 immunoreactivity. Endothelial cell staining for CXCL12 (brown) is seen in medulloblastoma-associated blood vessels (*Right*, arrow). (*b*) CXCR4 immunoreactivity (brown) is in GBM cells (*Left*) but not in an astrocyte of normal cortex (CTX) (*Center*, blue arrowhead). The low-power view of GBM (*Left*) reveals a densely cellular tumor composed of cells with fibrillary processes; the high-power view (*Inset*) shows immunoreactivity for CXCR4 in these cells. (*Center*) Low-power view of layers II and III of normal cerebral CTX; the high-power view (*Inset*) reveals a pyramidal neuron on the right, with weak CXCR4 immunostaining, and a cell with features of a nonreactive astrocyte (blue arrowhead) that is negative for CXCR4. Endothelial cell staining for CXCL12 (brown) is seen in GBM-associated blood vessel (*Right*). (*c*) CXCR4 (red) staining in tumor cells of a spontaneously arising medulloblastoma in a *ptc* +/− mouse (*Left*). CXCR4 immunoreactivity is not present in granule cells of the IGL. Nuclei are counterstained with DAPI. CXCL12 is localized to vascular endothelium of tumor-associated blood vessels. CXCL12 is in red, PECAM is in green (*Center*), and the merged image is in yellow (*Right*). An asterisk indicates the same blood vessel in each panel.

Statistical Analysis. Groups were compared by Student's *t* test (two-tailed) or by Fisher's analysis for nonparametric values.

All animal procedures were approved by the Dana–Farber Institutional Animal Care and Use Committee. All human tumor specimens were obtained and processed with the approval of Children's Hospital (Boston) and the Dana–Farber Cancer Institute Institutional Review Board.

Results

CXCR4 and CXCL12 Are Expressed in Human Brain Tumors. We examined CXCR4 and CXCL12 expression in pathological specimens of pediatric medulloblastomas, anaplastic astrocytomas, and GBMs. Nine of the 10 medulloblastoma samples examined were positive for CXCR4 immunoreactivity (Fig. 1*a*). In contrast, mature cerebellar granule cells, the normal cellular counterpart of medulloblastoma, exhibited little to no CXCR4 staining (Fig. 1*a*). Expression of CXCR4 was also evident in three of five anaplastic astrocytomas (data not shown) and five of five GBM specimens but not in astrocytes of the normal cortex (Fig. 1*b*).

Increased CXCR4 expression in tumors of neuronal and glial lineage was also evident in published pediatric brain tumor gene array data (20). From the list of all genes whose expression is greater in tumors than in normal cerebellum, we identified genes that encode growth factor receptors. In the RNA analyses, 5 of 8 medulloblastomas, 6 of 10 GBMs, and 3 of 6 supratentorial primitive neuroectodermal tumors exhibited greater *cxcr4* expression than normal cerebellum as established by standard signal-to-noise analysis (Fig. 5, which is published as supporting information on the PNAS web site) (20). *cxcr4* ranks eighth among all receptor genes in the consistency of its expression across tumor types and exhibits the second-greatest-fold mean difference in expression, 11.6, as compared with normal cerebellum. In comparison, *erbb2* and *pdgfra*, two receptors with well described roles in medulloblastoma and GBM (2, 3), exhibit a 1.7-fold and 3.4-fold increase in expression, respectively. Also up-regulated are several other mediators of survival, differentiation, and migration, including *vip2*, *ddr*, the retinoic acid receptor, and *trk3′*, and several receptors for inflammatory mediators, such as interleukins 6, 7, 8, and 13 and IFN-γ. Together, the immunohistochemical data and array analysis confirm that tumors of both neuronal and glial lineages express higher levels of CXCR4 than normal counterparts of their respective lineages.

CXCR4 is not known to be mutationally activated in cancer; therefore, its function in tumors is likely to require stimulation by its ligand CXCL12. In the CNS, CXCL12 is expressed by astrocytes (21, 22), neurons, and vascular endothelial cells (10). In 7 of the 10 pathological specimens of medulloblastoma we observed, CXCL12 immunostaining primarily localized to the vascular endothelium of tumor-associated blood vessels (Fig. 1*a*). Six of these also expressed CXCR4. Rarely, CXCL12 was also localized in scattered tumor cells. In addition to CXCR4 expression, all five GBM specimens displayed a vascular endothelial cell pattern of CXCL12 staining (Fig. 1*b*). Thus, a potential paracrine relationship for the activation of CXCR4 exists in malignant brain tumors of both neuronal and glial lineage.

This potential paracrine relationship is recapitulated in a spontaneously arising medulloblastoma from a mouse heterozygous for targeted deletion of the Shh receptor patched (*ptc* +/−). These mice serve as a model of Gorlin's syndrome (23). In both humans and mice with *ptc* mutations there is overactivity of the Shh pathway and an increased incidence of medulloblastoma (23, 24). Mouse medulloblastoma cells express CXCR4 (Fig. 1*c*), and tumor-associated blood vessels express CXCL12 (Fig. 1*c*). Mature granule cells of the internal granule cell layer are negative for CXCR4 expression (Fig. 1*c*), as previously described (10). Thus, high levels of CXCR4 expression are a common feature of adult and pediatric malignant brain tumors that is also present in mouse models of disease.

CXCL12 Stimulates and AMD 3100 Blocks Chemotaxis, Survival, and Proliferation in Medulloblastoma and GBM Cell Lines. To define the role of CXCR4 in brain tumor biology we examined expression and function of CXCR4 in tumor-derived cell lines both *in vitro* and *in vivo* (xenograft models). The Daoy medulloblastoma cell line and U87 GBM cell line express CXCR4 as revealed by immunofluorescent staining (Fig. 2*a*) and confirmed by RT-PCR and flow cytometry of fixed tumor cells (data not shown). Daoy and U87 cells demonstrated dose-dependent chemotactic responses to a gradient of CXCL12 (Fig. 2*b*). Chemotaxis of both cell lines could be blocked by pretreatment of cells with neutralizing antibodies to CXCR4 or pertussis toxin, indicating that these effects were mediated through CXCR4 and the activation of $G\alpha_i$ (7). Increased migration was not seen with a uniform distribution of CXCL12, indicating that this is a gradient-dependent chemotactic response (data not shown).

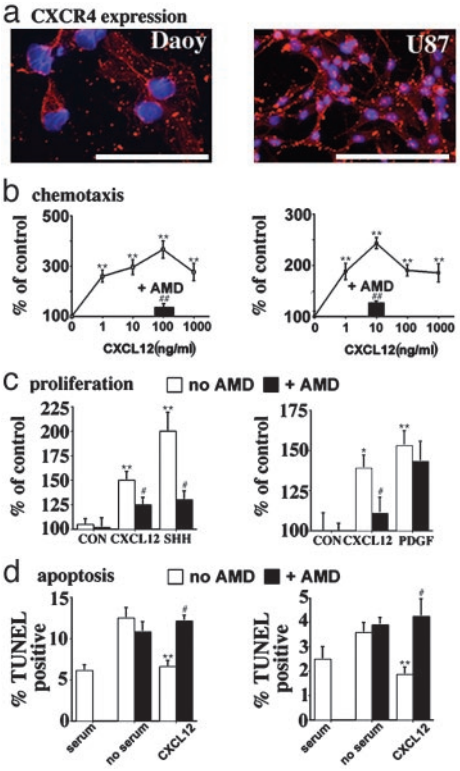

Fig. 2. Daoy and U87 cell responses to CXCL12 are blocked by AMD 3100 *in vitro*. Results with Daoy and U87 cells are shown in *Left* and *Right*, respectively. (*a*) CXCR4 expression in human tumor cell lines. U87 and Daoy cells exhibit punctate staining for CXCR4 (red). (*b*) CXCL12 is a chemoattractant for Daoy and U87 cells in a Boyden chamber assay. Peak CXCL12 chemotactic responses are blocked by AMD 3100 (solid bars). (*c*) CXCL12 and Shh are proliferative factors for Daoy cells (open bars), and CXCL12 and PDGF are proliferative factors for U87 cells (open bars). Proliferation in response to CXCL12 is inhibited by AMD 3100 in both cell lines, and AMD 3100 decreases Shh-induced proliferation in Daoy cells (solid bars). (*d*) The combination of SFM and CXCL12 is equivalent to serum-supplemented media in supporting cell survival (open bars). AMD 3100 blocked the survival effects of CXCL12 (solid bars). Each point represents the mean of three experiments done in triplicate. Data in *b* and *c* are mean percent changes relative to control ± SEM. Data in *d* are percentages TUNEL-positive cells ± SEM. *, $P < 0.05$; **, $P < 0.005$ (for the difference between SFM with and without CXCL12). #, $P < 0.05$; ##, $P < 0.005$ (for the effect of AMD 3100 on cells exposed to CXCL12). (Scale bars, 100 μm.)

Daoy and U87 cells depend on serum for maximal growth in culture. Twenty-four hours after serum withdrawal, each cell line exhibited a significant decrease in cell number. However, when serum was withdrawn in the presence of CXCL12 there was no decline in Daoy cell number, and U87 cell number declined by only 50%, indicating that CXCL12 has potent trophic effects on Daoy and U87 cells [Daoy cells in serum-supplemented media (SSM) = 100%, in serum-free media (SFM) = 79%, in CXCL12-supplemented SFM = 100%; U87 cells in SSM = 100%, in SFM = 77%, in CXCL12-supplemented SFM = 87%].

Because cell number represents a balance between proliferation and survival, we examined the effects of CXCL12 on each of these processes. In the presence of serum, CXCL12 (0.1 μg/ml) and Shh (1 μg/ml) led to a 50% and 100% increase in BrdUrd incorporation in Daoy cells, respectively (Fig. 2*c*). CXCL12 has previously been shown to be a proliferative factor for several glioma cell lines (15), and we confirmed that 1 μg/ml CXCL12 and 0.1 μg/ml PDGF each increased BrdUrd incorporation by 40–50% (Fig. 2*c*). The effects of CXCL12 on cell number are not exclusively caused by increased proliferation; CXCL12 also prevents tumor cell apoptosis. After 24 h in SFM,

both Daoy and U87 cells undergo increased apoptosis, and this is prevented by CXCL12 (Fig. 2*d*). Thus, CXCL12 is both a potent survival and proliferative factor for tumor cells with neuronal or glial characteristics.

AMD 3100 is a bicyclam noncompetitive antagonist of CXCL12 binding to CXCR4 (17). We asked whether AMD 3100 blocks the *in vitro* effects of CXCL12 on tumor cell growth, survival, and movement. CXCL12-induced chemotaxis of Daoy and U87 cells was decreased by 0.25 and 2.5 ng/ml AMD 3100, respectively (Fig. 2*b*). AMD 3100 was also effective at preventing CXCL12-induced proliferation of both cell lines (Fig. 2*c*). Interestingly, AMD 3100 also blocked Shh-induced proliferation in Daoy cells (Fig. 2*c*). The effect of AMD 3100 on Shh-induced proliferation was not the result of toxicity, because AMD 3100 alone did not produce a decrease in baseline proliferation. Nor did AMD 3100 appear to directly alter the Shh signaling pathway because it did not inhibit the effects of Shh on *ptc* expression, a transcriptional target of Shh signaling (data not shown). Because Shh can stimulate CXCR4 expression (25), these data suggest that Shh-induced increases in CXCR4 may be critical for Shh-dependent proliferation.

AMD 3100 inhibited CXCL12-induced proliferation of U87 cells but had no effect on PDGF-induced proliferation (Fig. 2*c*). In the absence of CXCL12, this same dose of AMD 3100 did not alter the rate of apoptosis (Fig. 2*d*). However, AMD 3100 completely blocked the survival effects of CXCL12 for both Daoy and U87 cells cultured in SFM (Fig. 2*d*). Together these data demonstrate that specific blockade of CXCR4 with AMD 3100 (26) abrogates the proliferative, antiapoptotic, and chemotactic effects of CXCL12 in these brain tumor cell lines.

In diverse cell types, CXCL12 stimulates proliferation and survival by activation of the Erk 1/2 and phosphatidylinositol 3-kinase pathways (27, 28). We used phosphospecific antibodies to Erk1/2 and Akt (protein kinase B) to determine whether these pathways are activated in response to CXCL12 in brain tumor cells. CXCL12 stimulates activation of Erk1/2 and Akt in both medulloblastoma and glioblastoma cells (Fig. 6, which is published as supporting information on the PNAS web site). In both Daoy and U87 cells, these rapid responses to CXCL12 are attenuated by AMD 3100.

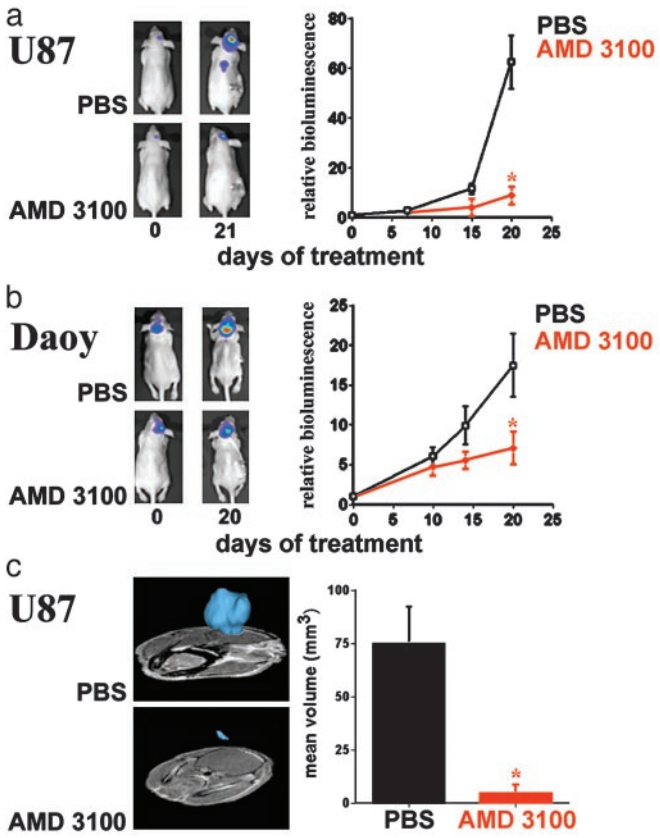

Fig. 3. AMD 3100 inhibits growth of intracranial U87 (*a* and *c*) and Daoy (*b*) xenografts. (*a* and *b*) Bioluminescent images from control and treated animals at the start and end of a 3-week treatment. Growth curves were derived from serial measurements in three experiments (four or five animals per treatment group per experiment). Data are mean values ± SEM. (*c*) Volumetric reconstructions of U87 intracranial xenografts (blue) after 3-week treatment. Tumor reconstructions are overlaid on coronal sections of the mouse brain. Volumes are mean values ± SEM for PBS and AMD 3100 treatment groups ($n = 4$). *, $P < 0.05$.

Generation and Characterization of Xenografts. Based on the expression of CXCL12 and CXCR4 in human tumors in conjunction with the *in vitro* effects of AMD 3100, we hypothesized that AMD 3100 might be an effective treatment for multiple malignant brain tumors, including medulloblastoma and GBM. We tested this hypothesis by using intracranial xenografts of Daoy and U87 cells that were engineered to express luciferase. This allowed noninvasive imaging of tumor-associated bioluminescence and quantification of tumor growth over time (29, 30). To evaluate the reliability of bioluminescence as a measure of tumor burden, we compared bioluminescence to volumetric measures derived from the 3D reconstruction of MRI images. There was a strong correlation between volumetric and bioluminescent measurements ($r = 0.977$). Thus, although bioluminescent images have limited utility in precise anatomic definition of tumor location, they do provide a good measure of tumor burden in a rapid, nonlethal, and noninvasive manner. Expression of luciferase, CXCR4, and CXCL12 was evaluated in intracranial xenografts, and, like native human tumors, the xenografts exhibited a potential paracrine relationship (Fig. 7, which is published as supporting information on the PNAS web site).

AMD 3100 Inhibits Xenograft Growth. Animals bearing established xenograft tumors with progressive growth during the postinjection period were separated into two groups. One group was treated with AMD 3100 at 0.24–0.36 mg/day, and the other was treated with PBS that was delivered to the subcutaneous tissue of the flank by osmotic pump for 1–21 days. Tumor burden as assessed by luminosity was grossly diminished in AMD 3100-treated animals compared with controls (Fig. 3 *a* and *b*). Growth curves derived from serial measurements of bioluminescence revealed a significant antineoplastic effect of AMD 3100 on U87 and Daoy xenografts. This was not caused by an effect of AMD 3100 on the expression or activity of luciferase, because significant and concordant differences in tumor volume were also evident in histological examination of tumors (data not shown) and in MRIs performed for one U87 xenograft study (Fig. 3*c*). Thus, differences between treatment groups reflect changes in tumor burden. Growth of GBM xenografts was similarly inhibited when AMD 3100 was administered by twice-daily, subcutaneous injections. There was no difference in mean body mass between groups, nor was there other evidence of drug-related toxicity (data not shown).

Within 24 h of initiating AMD 3100 treatment, apoptosis increased in tumor specimens from 1% to 1.36% ($P < 0.05$) (Fig. 4*a*). To determine whether the antitumor effects of AMD 3100 were caused by changes in apoptosis or proliferation or both, these parameters were analyzed in animals treated for 1 week with AMD 3100 or the vehicle. AMD 3100 had no effect on BrdUrd incorporation in GBM xenografts but did increase the rate of apoptosis from 1.2% to 2.6% (Fig. 4*b*). In contrast, medulloblastoma xenografts responded to AMD 3100 with a decrease in BrdUrd incorporation from 6.1% to 2.5% and an increase in apoptosis from 1.5%

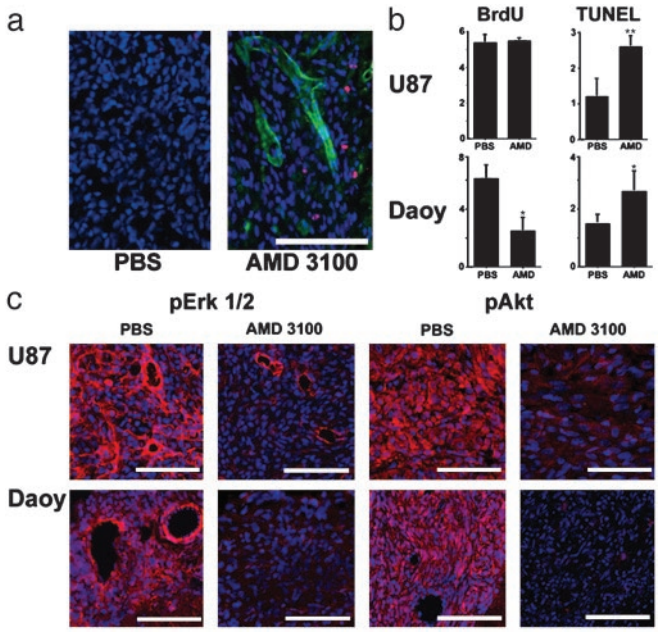

Fig. 4. AMD 3100 increases apoptosis and decreases activation of Erk 1/2 and Akt in tumor cells. (*a*) Apoptosis is increased in U87 xenografts within 24 h of AMD 3100 treatment compared to PBS control. Serial sections from AMD 3100-treated tumor were stained for PECAM (green) and TUNEL (red). Apoptosis was limited to tumor cells. Increases in apoptosis were also seen in U87 tumors analyzed at 48 h. (*b*) One week of AMD 3100 treatment increased U87 apoptosis without any change in proliferation. AMD 3100 treatment decreased proliferation and increased apoptosis in Daoy xenografts. Apoptosis was also increased in U87 tumors at 2 and 3 weeks of treatment (data not shown). Data presented are means ± SEM in two tumors per condition (1,000–5,000 cells per tumor). *, $P < 0.05$; **, $P < 0.005$. (*c*) U87 and Daoy xenografts immunostained for pErk 1/2 and pAkt. Immunopositivity of pErk 1/2 and pAkt was decreased in tumors treated for 3 weeks with AMD 3100 compared to those treated with PBS. (Scale bars, 100 μM.)

to 2.6% (Fig. 4*b*). There was limited infiltration of leukocytes into these tumors, and AMD 3100 had no effect on this (data not shown). Thus, AMD 3100 can function as a proapoptotic and an antiproliferative agent for brain tumors growing intracranially, leading to a decrease in tumor size.

The ability of CXCL12 to stimulate proliferation and survival is mediated by activation of the Erk 1/2 and phosphatidylinositol 3-kinase pathways in many cell types (27, 28). In medulloblastoma and GBM cells *in vitro*, CXCL12 stimulates both Erk 1/2 and Akt. To determine whether the effects of AMD 3100 on tumor growth reflect inhibition of CXCR4 signaling, we used phosphospecific antibodies to visualize pathway activation within the intracranial tumors. Tumor cells within growing medulloblastoma and glioblastoma xenografts displayed robust staining for phosphorylated Erk1/2 and Akt. In comparison, after three weeks of AMD 3100 treatment, immunostaining for both phosphorylated Erk 1/2 and Akt was markedly decreased in tumor cells (Fig. 4*c*) without any apparent change in overall levels of these kinases (data not shown). Decreased Erk1/2 and Akt activation was only seen within the tumor cells and not in the surrounding normal tissue or the endothelium of tumor-associated blood vessels. Taken together these data indicate that the ability of AMD 3100 to decrease tumor growth in animal models reflects direct inactivation of CXCR4 in tumor cells and consequent inhibition of Erk 1/2 and phosphatidylinositol 3-kinase pathways, resulting in increased tumor cell apoptosis and decreased proliferation.

Discussion

We have determined that malignant brain tumors of neuronal and glial lineage express high levels of CXCR4 and that small-molecule blockade of CXCR4 inhibits the growth of intracranial tumors. Previous studies have demonstrated CXCR4 and CXCL12 expression in adult GBM (14, 16). Here we show that CXCR4 and CXCL12 expression is also increased in pediatric GBM and medulloblastoma. Whereas diverse pathogenetic mechanisms function in the genesis of adult and pediatric GBM and medulloblastoma, CXCR4 appears to have an important role regardless of pathogenetic subtype or age of onset of disease.

In many medulloblastomas the high level of CXCR4 expression is likely to be a direct result of the oncogenic event. Gorlin's syndrome, a genetic disorder associated with increased risk of medulloblastoma, is caused by mutations in the *ptc* gene and consequent overactivity of the Shh pathway (23, 31). Studies in cerebellar GPCs have shown that activation of the Shh signaling pathway increases expression of *cxcr4* (25). CXCR4 expression is high in human tumors and in medulloblastomas from the *ptc* mutant mice. Thus, in many medulloblastomas, CXCR4 expression is likely to be a result of Shh pathway activation. Unlike medulloblastomas, glial tumors are not associated with increased Shh pathway activation. In these tumors, CXCR4 may instead be regulated by activation of the hypoxia-inducible factor (32) or NF-κB (33) pathways.

In vitro, CXCL12 regulates tumor cell proliferation, survival, and chemotaxis. Thus, *in vivo*, CXCL12/CXCR4 may contribute to the growth and spread of malignant brain tumors. In support of this hypothesis, treatment with AMD 3100, a small-molecule inhibitor of CXCR4, decreases the growth of intracranial xenografts. The effect of AMD 3100 on the growth of GBM xenografts was greater than that observed for medulloblastoma. This finding was surprising because AMD 3100 inhibited survival in GBM xenografts but decreased both proliferation and survival in medulloblastoma. Because AMD 3100 caused a 2.7-fold increase in apoptosis in GBM xenografts, but a 1.8-fold increase in apoptosis in medulloblastoma xenograft, the efficacy of AMD 3100 apparently correlates with the magnitude of its apoptotic effect. These studies suggest that CXCR4-mediated survival signaling contributes significantly to brain tumor biology and provide proof of concept for the blockade of CXCR4 as a therapeutic strategy in brain tumors

In addition to increasing apoptosis, the inhibition of CXCR4 by AMD 3100 blocked both CXCL12- and Shh-induced proliferation in medulloblastoma cells. This does not appear to reflect a direct effect of AMD 3100 on Shh signaling pathways. Instead, AMD 3100 inhibits activation of Erk 1/2 and Akt, mediators of CXCR4 that may be necessary for medulloblastoma cell proliferation in response to either CXCL12 or Shh. CXCL12 regulation of proliferation in astrocytes also involves the Erk 1/2 and phosphatidylinositol 3-kinase pathways (27, 34). Although AMD 3100 decreased the activation of both pathways, it did not reduce proliferation in GBM xenografts. Thus, the effects of AMD 3100 on GBM growth primarily reflect increased apoptosis.

The pattern of expression of CXCR4 and its ligand, CXCL12, in brain tumors establishes a potential paracrine loop that may be critical for tumor growth. Both GBM and medulloblastoma tumor cells express CXCR4, whereas CXCL12 is expressed by the endothelium of tumor-associated blood vessels. The ability of CXCR4 antagonists to decrease tumor growth *in vivo*, as shown here for GBM and medulloblastoma, may be selective for tumors in which there is ligand-initiated activation of CXCR4. Many other tumor types also express CXCR4 (39–45), and this receptor may contribute to the growth of diverse tumors that also produce high levels of the ligand.

The expression of CXCL12 in tumor blood vessels is also intriguing when considering the perivascular pattern of GBM growth (43). Our observations suggest that the chemoattraction of GBM cells to CXCL12-expressing vascular endothelium may contribute to this pattern. CXCL12 could also contribute to the

pattern of medulloblastoma spread. Medulloblastoma is distinctive among brain tumors in its capacity to metastasize to bone and liver tissue, which are rich sources of CXCL12.

Here, the importance of CXCL12 and CXCR4 to medulloblastoma and GBM biology was directly demonstrated through the antitumor activity of AMD 3100, a specific, noncompetitive antagonist of CXCL12 binding (17, 26). Although it is unclear whether AMD 3100 crosses an intact blood–brain barrier, tumors have abnormal blood–brain barrier function (44, 45). We found that AMD 3100 leads to increased tumor cell apoptosis within 24 h of the initiation in treatment, suggesting that it enters the intracranial tumor and acts directly on tumor cells. The safety of AMD 3100 has been established in clinical trials in which the drug was delivered either as a single dose (18) or as a continuous infusion. Side effects in 40 patients treated by continuous infusion (up to 160 $\mu g \cdot kg^{-1} \cdot hr^{-1}$ for several days) included paresthesia, gastrointestinal bloating, tachycardia, thrombocytopenia (one patient), ventricular premature beats (two patients) (G. Calandra, personal communication). This safety profile is encouraging for new clinical trials. The data presented here, demonstrating that AMD 3100 has a direct antitumor effect on GBMs and medulloblastoma, provide the scientific rationale for clinical evaluation of this or other CXCR4 antagonists in treating malignant brain tumors.

We thank N. Warrington, E. Tanner, R. Wright, M. Pazyra, E. Berry, T. Zolotarev, and E. Lin for technical assistance; Dr. P. Febbo for assistance with genomic analysis; Dr. A. Annuar for the gift of AMD 3100; Dr. O. Gilchrist for the gift of Shh protein; and Drs. G. Bridger, G. Calandra, J. Kim, C. Stiles, B. Rollins, and S. Pomeroy for helpful discussions. This work was supported by grants from the National Institutes of Health (to J.B.R., A.L.K., R.S.K., A.D.L., and R.A.S.), the Goldhirsh Foundation (to J.B.R. and A.L.K.), the Claudia Adams Barr Program (to A.L.K. and R.A.S.), the Whitaker Foundation and the Brigham Radiology Research and Education Fund (to Y.S. and K.S.), and the Stop and Shop Family Pediatric Brain Tumor Program (to M.W.K.).

1. Ries, L. A. G., Eisner, M. P., Kosary, C. L., Hankey, B. F., Miller, B. A., Clegg, L. & Edwards, B. K., eds. (2001) *SEER Cancer Statistics Review* (Natl. Cancer Inst., Bethesda).
2. Kleihues, P., Burger, P. C., Collins, V. P., Newcomb, E. W., Ohgaki, H. & Cavenee, W. K. (2000) in *World Health Organization Classification of Tumours: Pathology and Genetics of Tumours of the Central Nervous System*, eds. Kleihues, P. C. & Cavenee, W. K. (Int. Agency for Res. on Cancer, Lyon, France), pp. 29–39.
3. Giangaspero, F., Bigner, S. H., Kleihues, P., Pietsch, T. & Trojanowski, J. Q. (2000) in *World Health Organization Classification of Tumours: Pathology and Genetics of Tumours of the Central Nervous System*, eds. Kleihues, P. C. & Cavenee, W. K. (Int. Agency for Res. on Cancer, Lyon, France), pp. 129–137.
4. Luster, A. D. (1998) *N. Engl. J. Med.* **338,** 436–445.
5. Ma, Q., Jones, D., Borghesani, P. R., Segal, R. A., Nagasawa, T., Kishimoto, T., Bronson, R. T. & Springer, T. A. (1998) *Proc. Natl. Acad. Sci. USA* **95,** 9448–9453.
6. Zou, Y. R., Kottmann, A. H., Kuroda, M., Taniuchi, I. & Littman, D. R. (1998) *Nature* **393,** 595–599.
7. Klein, R. S., Rubin, J. B., Gibson, H. D., DeHaan, E. N., Alvarez-Hernandez, X., Segal, R. A. & Luster, A. D. (2001) *Development (Cambridge, U.K.)* **128,** 1971–1981.
8. Zhu, Y., Yu, T., Zhang, X. C., Nagasawa, T., Wu, J. Y. & Rao, Y. (2002) *Nat. Neurosci.* **5,** 719–720.
9. Lu, Q., Sun, E. E., Klein, R. S. & Flanagan, J. G. (2001) *Cell* **105,** 69–79.
10. Stumm, R. K., Rummel, J., Junker, V., Culmsee, C., Pfeiffer, M., Krieglstein, J., Hollt, V. & Schulz, S. (2002) *J. Neurosci.* **22,** 5865–5878.
11. Han, Y., Wang, J., He, T. & Ransohoff, R. M. (2001) *Brain Res.* **888,** 1–10.
12. Dorf, M. E., Berman, M. A., Tanabe, S., Heesen, M. & Luo, Y. (2000) *J. Neuroimmunol.* **111,** 109–121.
13. Bajetto, A., Bonavia, R., Barbero, S., Piccioli, P., Costa, A., Florio, T. & Schettini, G. (1999) *J. Neurochem.* **73,** 2348–2357.
14. Rempel, S. A., Dudas, S., Ge, S. & Gutierrez, J. A. (2000) *Clin. Cancer Res.* **6,** 102–111.
15. Sehgal, A., Keener, C., Boynton, A. L., Warrick, J. & Murphy, G. P. (1998) *J. Surg. Oncol.* **69,** 99–104.
16. Zhou, Y., Larsen, P. H., Hao, C. & Yong, V. W. (2002) *J. Biol. Chem.* **277,** 49481–49487.
17. Gerlach, L. O., Skerlj, R. T., Bridger, G. J. & Schwartz, T. W. (2001) *J. Biol. Chem.* **276,** 14153–14160.
18. Hendrix, C. W., Flexner, C., MacFarland, R. T., Giandomenico, C., Fuchs, E. J., Redpath, E., Bridger, G. & Henson, G. W. (2000) *Antimicrob. Agents Chemother.* **44,** 1667–1673.
19. Sun, Y., Zhou, J., Stayner, C., Munasinghe, J., Shen, X., Beier, D. R. & Albert, M. S. (2002) *Comp. Med.* **52,** 433–438.
20. Pomeroy, S. L., Tamayo, P., Gaasenbeek, M., Sturla, L. M., Angelo, M., McLaughlin, M. E., Kim, J. Y., Goumnerova, L. C., Black, P. M., Lau, C., *et al*. (2002) *Nature* **415,** 436–442.
21. Klein, R. S., Williams, K. C., Alvarez-Hernandez, X., Westmoreland, S., Force, T., Lackner, A. A. & Luster, A. D. (1999) *J. Immunol.* **163,** 1636–1646.
22. Rezaie, P., Trillo-Pazos, G., Everall, I. P. & Male, D. K. (2002) *Glia* **37,** 64–75.
23. Goodrich, L. V., Milenkovic, L., Higgins, K. M. & Scott, M. P. (1997) *Science* **277,** 1109–1113.
24. Evans, D. G., Farndon, P. A., Burnell, L. D., Gattamaneni, H. R. & Birch, J. M. (1991) *Br. J. Cancer* **64,** 959–961.
25. Zhao, Q., Kho, A., Kenney, A. M., Yuk Di, D. I., Kohane, I. & Rowitch, D. H. (2002) *Proc. Natl. Acad. Sci. USA* **99,** 5704–5709.
26. Hatse, S., Princen, K., Bridger, G., De Clercq, E. & Schols, D. (2002) *FEBS Lett.* **527,** 255–262.
27. Bajetto, A., Barbero, S., Bonavia, R., Piccioli, P., Pirani, P., Florio, T. & Schettini, G. (2001) *J. Neurochem.* **77,** 1226–1236.
28. Suzuki, Y., Rahman, M. & Mitsuya, H. (2001) *J. Immunol.* **167,** 3064–3073.
29. Rehemtulla, A., Stegman, L. D., Cardozo, S. J., Gupta, S., Hall, D. E., Contag, C. H. & Ross, B. D. (2000) *Neoplasia* **2,** 491–495.
30. Vooijs, M., Jonkers, J., Lyons, S. & Berns, A. (2002) *Cancer Res.* **62,** 1862–1867.
31. Vorechovsky, I., Tingby, O., Hartman, M., Stromberg, B., Nister, M., Collins, V. P. & Toftgard, R. (1997) *Oncogene* **15,** 361–366.
32. Lee, T. H., Avraham, H., Lee, S. H. & Avraham, S. (2002) *J. Biol. Chem.* **277,** 10445–10451.
33. Helbig, G., Christopherson, K. W., II, Bhat-Nakshatri, P., Kumar, S., Kishimoto, H., Miller, K. D., Broxmeyer, H. E. & Nakshatri, H. (2003) *J. Biol. Chem.* **278,** 21631–21638.
34. Barbero, S., Bonavia, R., Bajetto, A., Porcile, C., Pirani, P., Ravetti, J. L., Zona, G. L., Spaziante, R., Florio, T. & Schettini, G. (2003) *Cancer Res.* **63,** 1969–1974.
35. Libura, J., Drukala, J., Majka, M., Tomescu, O., Navenot, J. M., Kucia, M., Marquez, L., Peiper, S. C., Barr, F. G., Janowska-Wieczorek, A. & Ratajczak, M. Z. (2002) *Blood* **100,** 2597–2606.
36. Geminder, H., Sagi-Assif, O., Goldberg, L., Meshel, T., Rechavi, G., Witz, I. P. & Ben-Baruch, A. (2001) *J. Immunol.* **167,** 4747–4757.
37. Muller, A., Homey, B., Soto, H., Ge, N., Catron, D., Buchanan, M. E., McClanahan, T., Murphy, E., Yuan, W., Wagner, S. N., *et al*. (2001) *Nature* **410,** 50–56.
38. Schrader, A. J., Lechner, O., Templin, M., Dittmar, K. E., Machtens, S., Mengel, M., Probst-Kepper, M., Franzke, A., Wollensak, T., Gatzlaff, P., *et al*. (2002) *Br. J. Cancer* **86,** 1250–1256.
39. Koshiba, T., Hosotani, R., Miyamoto, Y., Ida, J., Tsuji, S., Nakajima, S., Kawaguchi, M., Kobayashi, H., Doi, R., Hori, T., *et al*. (2000) *Clin. Cancer Res.* **6,** 3530–3535.
40. Kijima, T., Maulik, G., Ma, P. C., Tibaldi, E. V., Turner, R. E., Rollins, B., Sattler, M., Johnson, B. E. & Salgia, R. (2002) *Cancer Res.* **62,** 6304–6311.
41. Payne, A. S. & Cornelius, L. A. (2002) *J. Invest. Dermatol.* **118,** 915–922.
42. Durig, J., Schmucker, U. & Duhrsen, U. (2001) *Leukemia* **15,** 752–756.
43. Scherer, H. J. (1938) *Am. J. Cancer* **34,** 333–351.
44. Davies, D. C. (2002) *J. Anat.* **200,** 639–646.
45. Seitz, R. J. & Wechsler, W. (1987) *Acta Neuropathol.* **73,** 145–152.